HEAVY FLAVOR PHYSICS FROM CLEO

Karen Lingel

Stanford Linear Accelerator Center

Abstract

The large dataset available at CLEO II is ideal for studying heavy flavor physics. We have searched for inclusive $b \to sg$ gluonic penguins. We have used an innovative method of neutrino reconstruction to measure $B \to (\pi/\rho/\omega)\ell\nu$ and $B \to D\ell\nu$. We also have observed new excited charm-strange baryons.

1 Introduction

The CLEO II detector [1] is operated at the Cornell Electron Storage Ring (CESR). The dataset consists of about 2.5 fb^{-1} taken at the $\Upsilon(4S)$ (on-resonance) and about 1.2 fb^{-1} taken at a center-of-mass energy about 35 MeV below $B\bar{B}$ threshold (off-resonance). Together the on- and off-resonance samples contain about 3.8 million $c\bar{c}$ events from continuum production. The on-resonance sample contains about 2.6 million $B\bar{B}$ events and the off-resonance sample is used as a B-free estimate of the continuum background.

The momentum of charged particles is measured in a tracking system consisting of three tracking devices: a 6-layer straw tube chamber, a 10-layer precision drift chamber, and a 51-layer main drift chamber, all operating inside a 1.5 T superconducting solenoid. The main drift chamber also provides a measurement of the specific ionization loss, dE/dx, used for particle identification. Additional particle identification is provided by time of flight (TOF) counters outside of the main drift chamber. Photons are detected using 7800 CsI crystals, which are also inside the magnet. Muons are identified using proportional counters placed at various depths in the steel return yoke of the magnet. The excellent efficiency and resolution of the CLEO II detector for both charged particles and photons are crucial in extracting signals and suppressing both continuum and combinatoric backgrounds.

2 $B \to \phi X_s$

There are several outstanding mysteries in B decay. First, the inclusive semileptonic branching fraction is experimentally measured to be $\mathcal{B}(B \to X\ell\nu) = (10.4 \pm 0.4)\%$ [2], lower than the theoretically preferred value of 12.5% [3]. Secondly, the number of charmed hadrons per B decay is experimentally measured to be $n_c = 1.10 \pm 0.06$ [2], whereas the theory predicts a value of $n_c \approx 1.3$ using the measured semileptonic branching fraction as input [2]. Figure 1 illustrates the discrepancy between the theoretical predictions and the experimental measurements. Thirdly, the number of B decays to two charmed quarks is measured to be $\mathcal{B}(b \to c\bar{c}s) = (15.6 \pm 2.7)\%$ [4], lower than the 30% predicted by theory.

It has been suggested that these three mysteries can be simultaneously solved by increasing the non-semileptonic, non-charm decay width of the B, for instance by increasing the rate of the gluonic penguin diagram $b \to sg$ [5]. New physics such as technicolor or supersymmetry can be introduced in such a way so as to increase the gluonic penguin rate, but to keep the electromagnetic penguin $b \to s\gamma$ rate within the measured bounds.

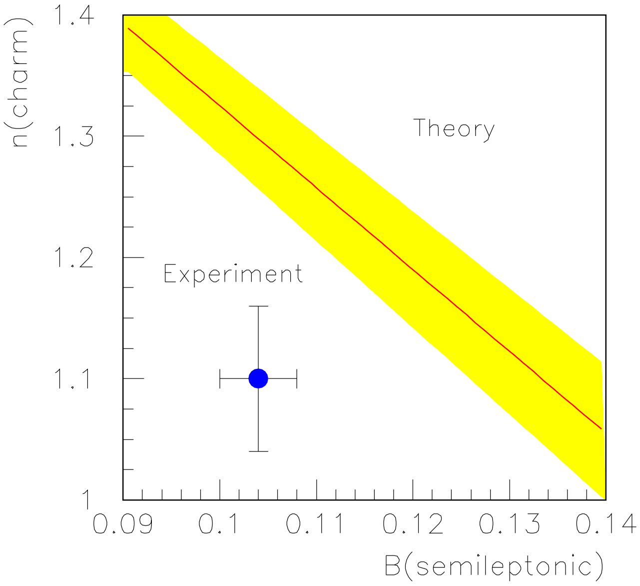

Figure 1: Number of charm per B decay (n_c) vs B semileptonic branching fraction. The experimental measurement is given by the point and the theoretical prediction is given by the shaded band.

A gluonic penguin rate of $\mathcal{O}(10\%)$ would be necessary to bring the theoretical predictions into agreement with the experimental measurements.

The decay $B \to \phi X_s$ is a good signature of the gluonic penguin (see Figure 2.) Exclusive searches for $B \to K\phi$ and $B \to K^*(892)\phi$ have been performed by CLEO, and there is no evidence for signals [6]. Deshpande, *et al.* [7] have calculated the inclusive rate $\mathcal{B}(B \to \phi X_s)$ to be $(0.6 - 2.0) \times 10^{-4}$, which is at least a factor of 10 higher than any of the individual exclusive modes. Therefore, it makes sense to perform an inclusive search. In addition, ϕ's are easy to find experimentally and ϕ's from $b \to c$ sources are Cabibbo-suppressed. On the other hand, the hadronization of the X_s is difficult to predict, which will lead to model dependence of the experimental efficiency. There is also plenty of ϕ background from continuum sources.

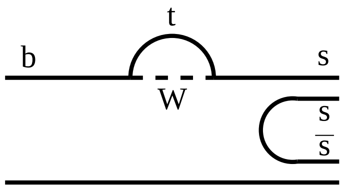

Figure 2: Hadronic penguin diagram for $B \to \phi X_s$.

CLEO has used two methods to search for $B \to \phi X_s$. The first is the momentum spectrum endpoint method. Continuum background is suppressed by utilizing the difference in event shape: B's are produced nearly at rest and decay isotropically, whereas lighter quarks (u, d, s, c) are produced with a high boost, and the events look jetty. The continuum-subtracted K^+K^- invariant mass is fitted for ϕ candidates with normalized momenta $x \equiv p_\phi/p_{\max}$ in the range $0.4 < x < 0.5$ ($\approx 2.07 < p_\phi < 2.60$ GeV). This is the momentum range expected for two-body $B \to \phi X_s$ decays, but higher than the momentum expected for ϕ's from $b \to c$ decays. The momentum endpoint method gives high reconstruction efficiency, but also high background.

The second method is the X_s reconstruction method. The ϕ is selected, along with a K or K_S^0, and 0 to 4 pions (including at most one π^0). The kaons and pions are selected so as to compose (with the ϕ) a B candidate with mass and energy near the mass and energy expected for a true B. As we are using the existence of the B candidate as a background suppression tool only, we are not concerned with mis-reconstruction or cross-feed. This method is a straight forward modification of a similar method used to measure the inclusive $b \to s\gamma$ branching fraction [8]. We require the mass of the reconstructed X_s be less than 2.0 GeV (which is equivalent to a ϕ momentum cut of approximately $p_\phi > 2.13$ GeV.) The ϕ candidate's K^+K^- invariant mass is then fitted separately for on- and off-resonance data. This method gives excellent background rejection, but also lower efficiency.

The fitted K^+K^- mass spectra are shown in Figures 3.1 and 3.2. The continuum subtracted ϕ yields and upper limits are given in Table 2. The reconstruction efficiencies (also given in Table 2) are calculated using three X_s hadronization models. The first assumes that the X_s is a mixture of equal amounts of the exclusive resonances K, $K^*(892)$, $K^*(1270)$, $K_1(1400)$, $K_1^*(1410)$, $K_2^*(1430)$, $K_0^*(1430)$, $K(1460)$, $K^*(1680)$, $K_2(1770)$, $K_3^*(1780)$, and $K_4^*(2045)$. The second model uses the exclusive resonances with the weights predicted by the phenomenological calculations of Davies *et al.*[9]. The third model uses predictions by Deshpande *et al.*[10] for the inclusive E_ϕ spectrum (with $p_F = 300$ MeV) and the X_s system is hadronized by JETSET 7.3 program [11] tuned to reproduce CLEO continuum data. Since this model does not include the $K\phi$ final state, a contribution of 6% is added to the model by hand. Each of the models gives similar efficiency, and the Deshpande *et al.* efficiencies are used to calculate upper limits.

No evidence of $B \to \phi X_s$ signals are seen in either method. Both methods give comparable upper limits, but the X_s reconstruction method gives a slightly better upper limit of $\mathcal{B}(B \to \phi X_s) < 1.3 \times 10^{-4}$, which rules out the upper region of the Deshpande *et al.* prediction: $(0.6 - 2.0) \times 10^{-4}$ [7].

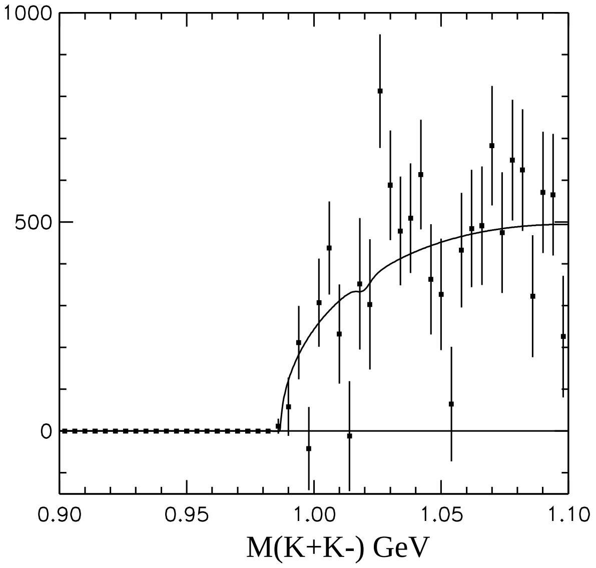

Figure 3.1: The continuum background subtracted K^+K^- mass distribution in the $b \to s$ gluon signal region for the endpoint analysis

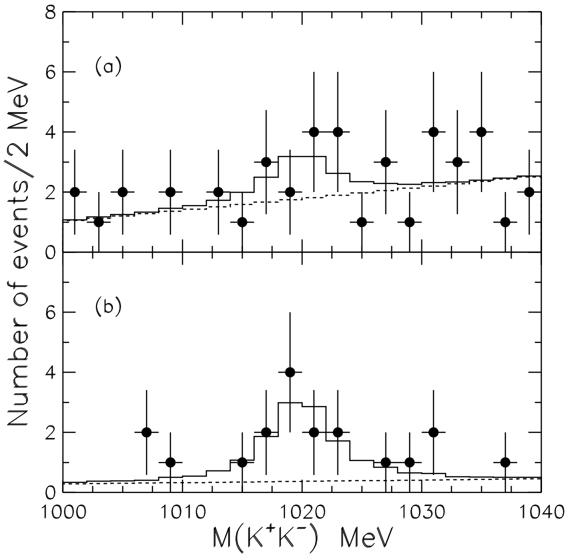

Figure 3.2: The K^+K^- mass distributions for the X_s reconstruction analysis for (a) on-resonance and (b) off-resonance data. The distributions are fit with a Monte Carlo ϕ shape and a linear background.

Table 1: Preliminary Results for $B \to \phi X_s$

Method	Endpoint	X_s recon
Yield	-57 ± 298	-5.8 ± 8.8
Yield limit	< 345	< 11.4
Efficiency (%)	68 ± 1	5.0 ± 0.2
av. resonance	66 ± 2.4	5.7 ± 1.7
Davies *et al.* [9]	68 ± 1	5.2 ± 0.1
Deshpande *et al.* [10]	68 ± 1	5.0 ± 0.2
$\Delta\mathcal{B}$	$< 2.2 \times 10^{-4}$	$< 1.1 \times 10^{-4}$
	(for $0.4 < x < 0.5$)	(for $M_{X_s} < 2$ GeV)
$\mathcal{B}$ (Deshpande *et al.*[10])	$< 2.3 \times 10^{-4}$	$< 1.3 \times 10^{-4}$

3 Exclusive $b \to u\ell\nu$ decays

Both CLEO [12] and ARGUS [13] have extracted $|V_{ub}|$ by observing leptons from B decays above the kinematic momentum limit for $b \to c$ decays ($2.3 < p_\ell < 2.6$ GeV). However, the large extrapolation from the endpoint region to the full momentum spectrum introduces large theoretical uncertainty, in fact, the value of $|V_{ub}|$ varies almost a factor of two amongst different theoretical models. Alternatively, we can extract $|V_{ub}|$ by measuring exclusive $b \to u\ell\nu$ modes.

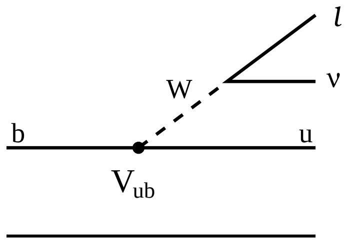

Figure 3: Feynman diagram for $b \to u\ell\nu$.

The excellent hermeticity and efficiency of the CLEO II detector allow us to reconstruct the undetected momentum and energy of a neutrino by using the missing momentum and energy of the event. We take care to eliminate falsely reconstructed tracks and showers, and to remove events which are likely to have additional unreconstructed particles (events with more than one lepton, events with non-zero total charge). We require that the invariant mass of the neutrino candidate be consistent with 0. Using these criteria, we find that the resolution of the neutrino momentum is 110 MeV and the resolution of the neutrino energy is 260 MeV.

Once a neutrino candidate is found, we can fully reconstruct a B candidate using $E_\nu = |\overrightarrow{p_\nu}| = |\overrightarrow{p_{\rm miss}}|$. We search for the five modes $\pi^-\ell^+\nu$, $\pi^0\ell^+\nu$, $\rho^-\ell^+\nu$, $\rho^0\ell^+\nu$, and $\omega\ell^+\nu$. Since each B is produced with half the center-of-mass energy, we construct the energy difference of the B candidate $\Delta E \equiv E_{\rm beam} - (E_h + E_\ell + |\overrightarrow{p_\nu}|)$, where h is the hadron candidate. We reconstruct the beam-constrained mass $M = \sqrt{E^2_{\rm beam} - |\overrightarrow{p_h} + \overrightarrow{p_\ell} + \overrightarrow{p_\nu}|^2}$. To determine the signal yields, we fit the distributions in the $M - \Delta E$ plane for the five modes simultaneously, using isospin relations to constrain the neutral meson rates relative to the charged meson rates: $\frac{1}{2}\Gamma(B^0 \to \pi^-\ell^+\nu) = \Gamma(B^+ \to \pi^0\ell^+\nu)$ and $\frac{1}{2}\Gamma(B^0 \to \rho^-\ell^+\nu) = \Gamma(B^+ \to \rho^0\ell^+\nu) = \Gamma(B^+ \to \omega\ell^+\nu)$. The simultaneous fit allows us to constrain cross-feed between modes. Projections of the fit onto the M axis are shown in Figure 4. Preliminary results for branching fractions, the ratio of ρ and π branching fractions and $|V_{ub}|$ (using the π branching fractions) are given in Table 3. The WSB [15] and ISGW-2 [17] models predict ρ/π ratios in good agreement with the experimental measurement, while the ISGW [14] and KS [16] models are in poorer agreement, but because the experimental errors are non-Gaussian and asymmetric, no model is experimentally ruled out.

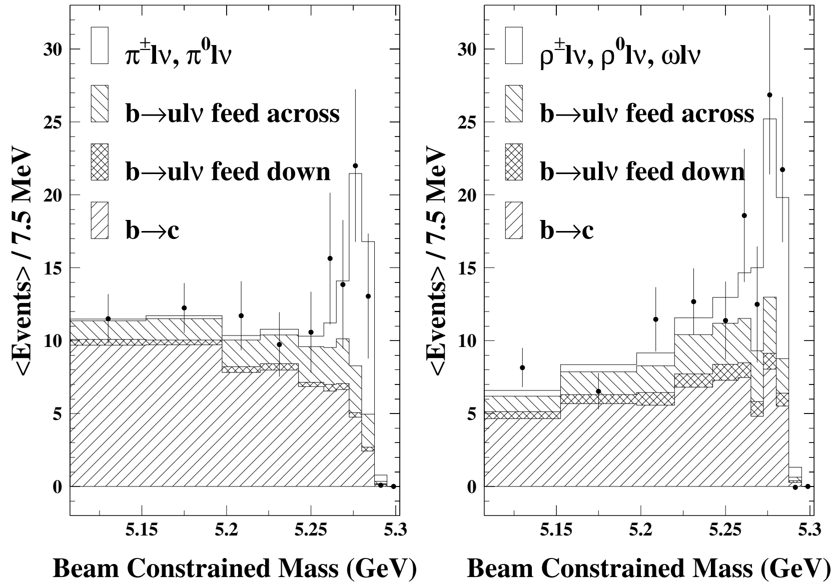

Figure 4: Beam-constrained mass distributions for combined $\pi^-\ell^+\nu$ and $\pi^0\ell^+\nu$ modes (left) and the combined $\rho^-\ell^+\nu$, $\rho^0\ell^+\nu$ and $\omega\ell^+\nu$ modes (right). The points are continuum- and fake-subtracted data. The histograms show the results of the fit for background from $b \to c$, feed-down from higher mass $b \to u\ell\nu$, signal mode cross-feed, and signal.

Table 2: Preliminary results from $B \to (\pi/\rho/\omega)\ell\nu$.

Model	$\mathcal{B}(B^0 \to \pi^-\ell^+\nu)$ (10^{-4})	$\mathcal{B}(B^0 \to \rho^-\ell^+\nu)$ (10^{-4})	$\Gamma(\rho\ell\nu)/\Gamma(\pi\ell\nu)$ Measured	$\Gamma(\rho\ell\nu)/\Gamma(\pi\ell\nu)$ Pred.	V_{ub} (π) (10^{-3})
ISGW [14]	$1.34 \pm 0.35 \pm 0.28$	$2.28 \pm 0.36 \pm 0.59$	$1.70^{+0.81}_{-0.50} \pm 0.58$	4.0	6.3 ± 1.06
WSB [15]	$1.63 \pm 0.46 \pm 0.34$	$3.88 \pm 0.54 \pm 1.01$	$2.39^{+1.18}_{-0.69} \pm 0.81$	3.0-4.3	3.7 ± 0.64
KS [16]	$1.56 \pm 0.43 \pm 0.33$	$2.69 \pm 0.35 \pm 0.70$	$1.72^{+0.79}_{-0.47} \pm 0.58$	4.6	3.7 ± 0.64
ISGW-2 [17]	$1.98 \pm 0.51 \pm 0.42$	$3.16 \pm 0.45 \pm 0.82$	$1.59^{+0.70}_{-0.44} \pm 0.54$	1.5	3.6 ± 0.60

4 $B^- \to D^0 \ell^- \bar{\nu}$

It is possible to apply the neutrino reconstruction technique to additional semileptonic decays. A natural choice is $B \to D\ell\nu$. In the traditional missing-mass technique, the B is approximated to have zero momentum, and the candidate neutrino mass ($\equiv$ missing mass) is then determined using the energies and momenta of the reconstructed D and ℓ. Candidates with $M_\nu \approx 0$ are kept. The missing mass technique works well for $B \to D^*\ell\nu$ decays, where the $D^* \to D\pi$ or $D^* \to D\gamma$ decay provides an additional background-reducing constraint. However, the missing mass method presents some difficulties when applied to $D\ell\nu$. There is enormous background from $D^*\ell\nu$ and $D^{**}\ell\nu$ decays where the soft pions or photons from the D^*/D^{**} decays are missed, and their momenta and energies are attributed to the neutrino candidates. Since the B is not at rest, but has momentum $\approx$ 300 MeV, the missing mass resolution is quite large, so it is difficult to distinguish decays with a missing neutrino plus a missing soft particle from decays with only a missing neutrino. The neutrino reconstruction technique, since it uses information from the entire $B\bar{B}$ event rather than a single candidate B, will reduce background from $D^*\ell\nu$ and $D^{**}\ell\nu$.

The energy and momentum of a B candidate is reconstructed using the measured energy and momenta of the D and ℓ candidates and using $E_\nu = |\overrightarrow{p_\nu}| = |\overrightarrow{p_{\rm miss}}|$, where $\overrightarrow{p_{\rm miss}}$ is the missing momentum of the event. The neutrino candidate is required to have mass consistent with 0. Background from $D^*\ell\nu$ is reduced by making explicit $D^0\pi$ and $D^0\gamma$ mass vetos. The B candidate is required to have energy consistent with $E_{\rm beam}$. Figure 5 shows the beam-constrained mass distribution for candidate events, as well as background estimates (from Monte Carlo, normalized to CLEO branching fractions) from $D^*\ell\nu$. The preliminary branching fraction is measured to be $\mathcal{B}(B^- \to D^0\ell^-\bar{\nu}) = (1.95 \pm 0.29 \pm 0.47)\%$.

5 Excited Charm Strange Baryons

One of the highlights of the charm physics program at CLEO is the discovery of new excited charm strange baryons [18]. In the Ξ_c system, the ground state particles, Ξ_c^+ and Ξ_c^0 have $J^P = \frac{1}{2}^+$, and the spin of the light di-quark is 0. The next highest states are expected to be the $J^P = \frac{1}{2}^+$ Ξ_c' and $J^P = \frac{3}{2}^+$ Ξ_c^* states, where the light di-quark is in a spin $= 1$ configuration. The Ξ_c' states are expected [19] to have mass below $\Xi_c\pi$ threshold, and thus will decay electromagnetically to $\Xi_c\gamma$. In fact, there is a preliminary result from

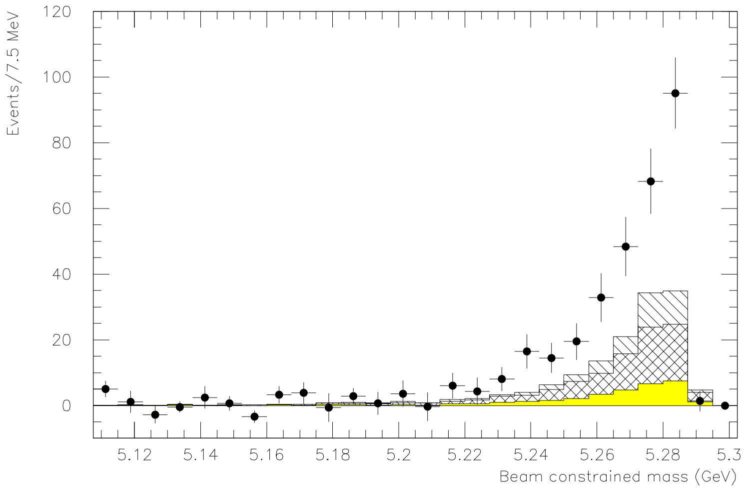

Figure 5: Preliminary beam-constrained mass spectra for continuum- and D^0 sideband background-subtracted data (points) and backgrounds from $B \to D^* \ell \nu$: $D^{*0} \to D^0 \gamma$ (hatched), $D^{*0} \to D^0 \pi^0$ (cross-hatched), and $D^{*-} \to D^0 \pi^-$ (shaded).

WA89 indicating a possible signal in $\Xi_c^{\prime +} \to \Xi_c^+ \gamma$ with a mass difference of about 95 MeV [20]. On the other hand, the Ξ_c^* states are expected to be above $\Xi_c \pi$ threshold.

CLEO has searched for $\Xi_c^+ \pi^-$ and $\Xi_c^0 \pi^+$ combinations, with the following Ξ_c decay modes:

$\Xi_c^+ \to \Xi^- \pi^+ \pi^+ \quad (\Xi^- \to \Lambda \pi^-, \Lambda \to p \pi^-)$
$\Xi_c^+ \to \Xi^0 \pi^+ \pi^0 \quad (\Xi^0 \to \Lambda \pi^0, \Lambda \to p \pi^-)$
$\Xi_c^+ \to \Sigma^+ K^{*0} \quad (\Sigma^+ \to p \pi^0, K^{*0} \to K^- \pi^+)$
$\Xi_c^0 \to \Xi^- \pi^+ \quad (\Xi^- \to \Lambda \pi^-, \Lambda \to p \pi^-)$
$\Xi_c^0 \to \Omega^- K^+ \quad (\Omega^- \to \Lambda K^-, \Lambda \to p \pi^-)$
$\Xi_c^0 \to \Xi^- \pi^+ \pi^0 \quad (\Xi^- \to \Lambda \pi^-, \Lambda \to p \pi^-)$
$\Xi_c^0 \to \Xi^0 \pi^+ \pi^- \quad (\Xi^0 \to \Lambda \pi^0, \Lambda \to p \pi^-)$

The mass difference spectra are shown in Figures 6 and 7. We find mass differences of $M(\Xi_c^+ \pi^-) - M(\Xi_c^+) = 178.2 \pm 0.5 \pm 1.0$ MeV and $M(\Xi_c^0 \pi^+) - M(\Xi_c^0) = 174.3 \pm 0.5 \pm 1.0$ MeV. Both states are quite narrow, and we find upper limits on the intrinsic widths: $\Gamma(\Xi_c^+ \pi^-) < 5.5$ MeV and $\Gamma(\Xi_c^0 \pi^+) < 3.1$ MeV. We identify these states as the Ξ_c^* states because the masses and widths of the states are consistent with theoretical predictions for Ξ_c^* states and inconsistent with the predictions for Ξ_c' [19]. The states are also inconsistent with the preliminary measurement of the $\Xi_c^{\prime +}$ state reported by WA89.

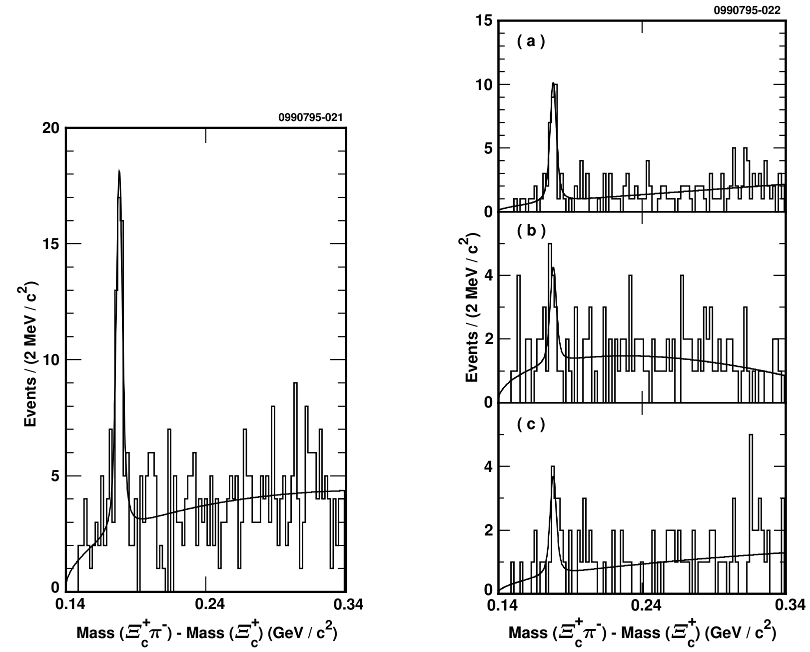

Figure 6: The spectra of the mass difference $M(\Xi_c^+\pi^-) - M(\Xi_c^+)$ for the combined Ξ_c^+ decay modes (left) and for the Ξ_c^+ decay modes separately (right): (a) $\Xi^-\pi^+\pi^+$, (b) $\Xi^0\pi^+\pi^0$, and (c) Σ^+K^{*0}.

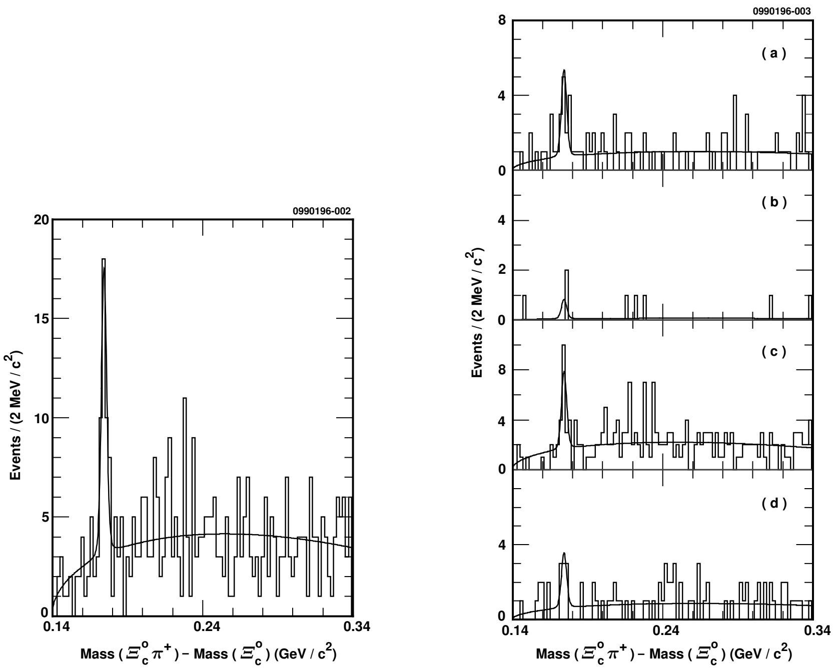

Figure 7: The spectra of the mass difference $M(\Xi_c^0\pi^+) - M(\Xi_c^0)$ for the combined Ξ_c^0 decay modes (left) and for the Ξ_c^0 decay modes separately (right): (a) $\Xi^-\pi^+$, (b) Ω^-K^+, (c) $\Xi^-\pi^+\pi^0$, and (d) $\Xi^0\pi^+\pi^-$.

6 Summary

There are many heavy flavor analyses ongoing at CLEO, utilizing the large charm and B data samples. Only highlights of the heavy flavor physics program could be mentioned here. We have searched for evidence of gluonic penguins inclusively in the mode $B \to \phi X_s$, and have no evidence for signals. We have used a neutrino reconstruction technique to observe signals in exclusive $b \to u\ell\nu$ modes, and have made new measurements of $|V_{ub}|$. The neutrino reconstruction technique has been used to make a new measurement of $B^- \to D^0 \ell^- \bar{\nu}$. We have observed excited charm-strange baryons, which we interpret as Ξ_c^*

Acknowledgments

I thank my CLEO colleagues, especially Tom Browder, Tomasz Skwarnicki, Lawrence Gibbons, Ed Thorndike, Ken Bloom, Persis Drell, John Yelton, and Rob Kutschke. We gratefully acknowledge the effort of the CESR staff in providing us with excellent luminosity and running conditions. This work was supported by the National Science Foundation, the U.S. Department of Energy, the Heisenberg Foundation, the Alexander von Humboldt Stiftung, the Natural Sciences and Engineering Research Council of Canada and the A.P. Sloan Foundation.

References

[1] Y. Kubota, *et al.*, Nucl. Instrum. Methods Phys. Res. Sect. A **320**, 66 (1992).

[2] G. Buchalla, I. Dunietz, and H. Yamamoto, Phys. Lett. **B364**, 188 (1995).

[3] G. Altarelli and S. Petrarca, Phys. Lett. **B261**, 303 (1991); I. I. Bigi, *et al.*, Phys. Lett. **323**, 408 (1994); A. F. Falk, M. B. Wise, and I. Dunietz, Phys. Rev. **D51**, 1183 (1995); E. Bagan, *et al.*, Nucl. Phys. **B432**, 3 (1994); E. Bagan, *et al.*, Phys. Lett. **B342**, 362 (1995); E. Bagan, *et al.*, Phys. Lett. **B351**, 546 (1995); M. B. Voloshin, Phys. Rev. **D51**, 3948 (1995); I. Dunietz, FERMILAB-PUB-94/361-T, hep-ph/9503414 (Jan. 1995).

[4] T. E. Browder and K. Honscheid, Progress in Particle and Nuclear Physics, **35**, ed. K. Faessler.

[5] A. Kagan, Phys. Rev. **D51**, 6196 (1995).

[6] CLEO Collaboration (D. M. Asner, *et al.*), Phys. Rev. **D53**, 1039 (1996).

[7] N. G. Deshpande and X.-G. He, Phys. Lett. **b336**, 471 (1994); Proceedings of the 27$^{\text{th}}$ International Conference on High Energy Physics, Glasgow, Scotland, 20-27 July 1994, eds. P. J. Bussey and I. G. Knowles, Institute of Physics Publishing, p. 1311; also Univ. of Oregon Report OITS-555, (1994).

[8] CLEO Collaboration (M. S. Alam, *et al.*), Phys. Rev. Lett. **74** 3113 (1995).

[9] A. J. Davies, *et al.*, Phys. Rev. D49, 5882 (1994).

[10] N. G. Deshpande, *et al.*, Univ. of Oregon Report OITS-555 (1994).

[11] T. Sjöstrand, Computer Physics Commun. **39**, 347 (1986); T. Sjöstrand and M. Bengtsson, Computer Physics Commun. **43**, 367 (1987).

[12] CLEO Collaboration (R. Fulton, *et al.*), Phys. Rev. Lett. **64**, 16 (1990); CLEO Collaboration (J. Bartelt, *et al.*), Phys. Rev. Lett. **71**, 4111 (1993).

[13] ARGUS Collaboration (H. Albrecht, *et al.*), Phys. Lett. **B234** 409 (1990); ARGUS Collaboration (H. Albrecht, *et al.*), Phys. Lett. **B255** 297 (1991).

[14] N. Isgur, *et al.*, Phys. Rev. **D39**, 799 (1989).

[15] M. Wirbel, B. Stech, and M. Bauer, Zeit. Phys. **C29**, 637 (1985).

[16] J. G. Körner and G. A. Schuler, Zeit. Phys. **C38**, 511 (1988).

[17] N. Isgur and D. Scora, CEBAF Report CEBAF-TH-94-14 (1994).

[18] CLEO Collaboration, (P. Avery, *et al.*), Cornell Report CLNS 95/1352, CLEO 95-14; CLEO Collaboration, (L. Gibbons, *et al.*), Cornell Report CLNS 96/1394, CLEO 96-4.

[19] J. Richard and P. Taxil, Phys. Lett. **B128**, 453 (1983); S. Fleck and J. Richard, Particle World **1**, 67 (1990); J. Korner and H. Siebert, Ann. Rev. of Nucl. and Part. Science, **41**, 511 (1991); P. Geiger and R. Cutkosky, Phys. Rev. **D48**, 1315 (1993); K. Maltman and N. Isgur, Phys. Rev. **D22**, 1701 (1980).

[20] R. Werding, "Production of Charmed Baryons in the CERN Hyperon Beam Experiment WA89", talk presented at ICHEP Conference, Glasgow, 1994.